

Investigation of Aggregation-Induced Phosphorescence of Non-Symmetric [Pt(C[^]N^{*}N[^]C['])] Complexes in Block Copolymer Micelles: Effects of Pt(II) Complex and Micellar Core

Nina A. Zharskaia,^[a] Elizaveta V. Durova,^[a] Anastasia I. Solomatina,^[a] Anastasia A. Elistratova,^[a] Petr S. Vlasov,^[a] Ekaterina E. Galenko,^[a] Alexander F. Khlebnikov,^[a] Sergey P. Tunik,^{*[a]} and Pavel S. Chelushkin^{*[a]}

The aggregation-induced phosphorescence emission (AIPE) phenomenon (emergence or increase in phosphorescence intensity as a result of aggregation of phosphorescent emitters) is regarded nowadays as an effective tool for improving brightness and tuning photophysical properties of phosphors. The intrinsic drawback of the aggregates featuring AIPE—their instability in aqueous dispersions, which hampers their utility in biomedical applications—can be overcome by their stabilization inside block copolymer micelles. Herein, we investigate the effects of both ligand and micellar core chemistries on the emergence of

AIPE by using a series of the [Pt(C[^]N^{*}N[^]C['])] complexes embedded into three block copolymers with different micellar cores. It has been shown that the only micelles that supported AIPE revealed for the corresponding complexes in solid state are those with poly(ϵ -caprolactone) cores. The latter observation can be explained by the ability of poly(ϵ -caprolactone) to demonstrate non-negligible swelling in water, the content of which in the micellar core formed by this polymer seems to be high enough to induce the aggregation of the complexes and the concomitant AIPE effect.


1. Introduction

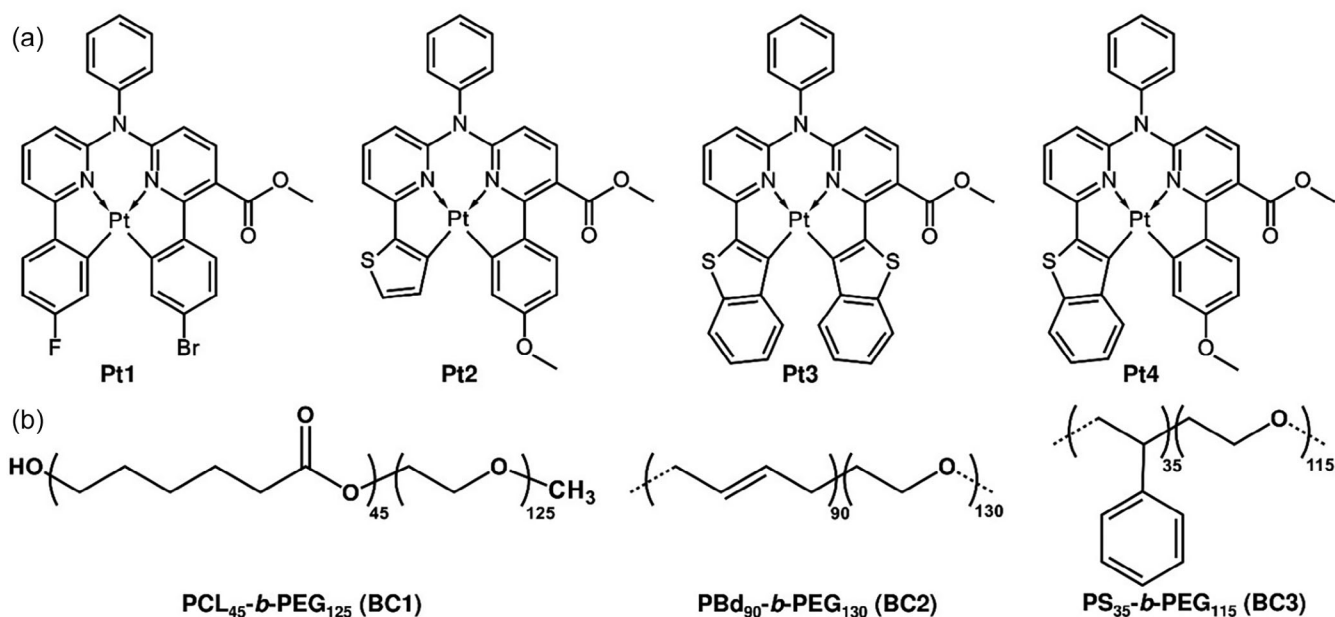
The effect of aggregation-induced phosphorescence emission, abbreviated as AIPE, consists in emergence (ignition) of phosphorescence or increase in phosphorescence intensity due to aggregation of phosphors, primarily represented by transition metal complexes (TMC).^[1,2] Currently, this effect is regarded as an effective tool for improving the brightness of phosphors due to suppression of non-radiative relaxation channels upon aggregation.^[1,2] Additionally, in the case of TMC prone to metallophilic interactions (e.g., square-planar Pt(II),^[3–6] Pd(II),^[7] and Rh(I)^[8,9] complexes), it can also be used for tuning such photophysical properties as absorption and emission energy of the phosphors. Indeed, the aggregation of above-mentioned complexes very often induces metal–metal bonding that leads to formation of the MMLCT excited states, which commonly give lower energy gap between excited and ground states.^[1,2] As a result, emission and/or excitation bands display bathochromic shifts that can ultimately generate rather intense near-infrared (NIR) phosphorescence, which is very promising in various bioimaging applications (e.g., as intracellular organelle trackers or biosen-

sors). In these experiments, emission in the so-called “biological window of transparency” (650–900 nm) is of critical importance for detection of signals in living tissues.^[10] In this context, it is worth noting that quantum yield (QY) and brightness of NIR emitters usually suffer from the so-called “energy gap law”^[11–13] that implies easy vibrational non-radiative relaxation of emissive excited states thereby strongly decreasing luminescence QY. However, this common drawback of NIR emitters can be effectively overcome in the aggregated chromophores, thus making possible their application in QY-demanding experiments.

The AIPE phenomenon is typically manifested in either the condensed phase (crystals,^[1,2] polymer films,^[14–16] or ground powders^[17]), where aggregation is supported by solid-state packing or in nanoparticles^[1,2,17] formed by mixing the organic solutions of hydrophobic AIPE-active emitters (often called AIPEgens) with water. These nanoaggregates could be a convenient form of using the AIPEgens in biomedical applications, but their poor colloidal stability in aqueous dispersions hampers their use in this field. To solve this problem, several research groups proposed the aggregate stabilization in uniform^[18] or two-layered core-shell^[19] polymer nanoparticles. Recently, our group demonstrated^[20] an alternative way for AIPEgens stabilization inside block copolymer micelles^[21,22] formed by diblock copolymer of ϵ -caprolactone and ethylene glycol, PCL₄₅-*b*-PEG₁₁₅, which effectively stabilized the aggregates of the [Pt(C[^]N^{*}N[^]C['])] complexes, preserved AIPE, and demonstrated high potential for their application as oxygen nanosensors. To date, the ability of polymer micelles to stabilize aggregates of phosphorescent AIPEgens is demonstrated only in the above-mentioned study^[20] despite numerous reports on the stabilization of fluorescent organic AIPEgens by various types of micelles, including the poly-

[a] N. A. Zharskaia, E. V. Durova, Dr. A. I. Solomatina, A. A. Elistratova, P. S. Vlasov, Dr. E. E. Galenko, Prof. A. F. Khlebnikov, Prof. S. P. Tunik, Dr. P. S. Chelushkin
Institute of Chemistry, St. Petersburg State University, Universitetskii Av. 26, St. Petersburg 198504, Russia
E-mail: sergey.tunik@spbu.ru
p.chelushkin@spbu.ru

 Supporting information for this article is available on the WWW under <https://doi.org/10.1002/slct.202405683>



Scheme 1. Chemical structures of Pt1–Pt4 complexes (a) and block BC1–BC3 copolymers (b) used in the study.

mer ones.^[23] In this context, the question of how general is the observed effect of AIPE generation via embedding the AIPEgens into polymer micelles still remains unclear. To answer this question, we investigate the influence of block copolymer nature and properties of the [Pt(C[∗]N[∗]N[∗]C[∗])] complexes on the emergence of AIPE using a series of phosphorescent block copolymer micelles, which includes three block copolymers with almost identical hydrophilic blocks and three different hydrophobic blocks loaded by four different [Pt(C[∗]N[∗]N[∗]C[∗])] complexes, see Scheme 1.

2. Results and Discussion

2.1. Design of the Study and Characterization of Starting Compounds

Encapsulation of the Pt(II) complexes into block copolymer micelles implies that the AIPEgens get buried and aggregated inside a hydrophobic micellar core, which means that the emergence of AIPE should strongly depend on interactions between AIPEgens and hydrophobic blocks. A straightforward way of tuning these interactions is changing the chemical nature of both entities that prompted us to perform the investigation of the effects of tetradentate C[∗]N[∗]N[∗]C[∗] ligands in the [Pt(C[∗]N[∗]N[∗]C[∗])] complexes and hydrophobic (core-forming) blocks on the emergence and magnitude of AIPE.

To vary the properties of AIPEgens, we used a series of four Pt(II) complexes, Pt1–Pt4 (Scheme 1a), that were recently obtained and characterized in our group.^[17] The complexes Pt1–Pt4 differ in the structure of the metalating functions in the tetradentate C[∗]N[∗]N[∗]C[∗] ligands. The key feature of this series is that two complexes, namely Pt1 and Pt2, display AIPE in the water/tetrahydrofuran (THF) mixtures or in solid state upon

grinding of crystals, while the Pt3 and Pt4 complexes are not AIPE-active under these conditions.^[17] Moreover, in our follow-up work, we demonstrated that the aggregates of AIPE-active [Pt(C[∗]N[∗]N[∗]C[∗])] complex, similar to Pt1 and Pt2, are effectively stabilized inside the cores of polymer micelles formed by PCL₄₅-*b*-PEG₁₁₅ block copolymer and show a pronounced AIPE.^[20]

The Pt1–Pt4 complexes were prepared using the previously published protocols.^[17] However, upon crystallization of freshly synthesized portions of Pt1 from the THF/pentane system we revealed a novel allotropic modification, a “yellow” crystalline form, in addition to the “green” crystals reported earlier.^[17] The newly obtained “yellow” allotrope gave single crystals suitable for XRD analysis. Crystallographic data and key structural parameters of the “yellow” allotrope are summarized in Tables S1 and S2; molecular views and crystal cell packing patterns are shown in Figure S1. In crystal cell, both allotropes display pairwise intermolecular stacking due to $\pi-\pi$ interaction between ligands aromatic systems, see Figure S1D–F with the shortest $\pi-\pi$ contacts of ca. 3.4 Å. The obtained structural parameters are not exceptional for the compounds of this type^[17] though Pt–Pt distances in the pairs of the “yellow” form (5.622 Å) are substantially shorter than those for the “green” form (6.022 Å^[17]) but still are well above the sum of platinum van der Waals radii (ca. 3.5 Å). Nevertheless, a substantially smaller deviation from planar geometry (dihedral angles between adjacent coordinated fluorophenyl and bromophenyl rings were 25.21° for the “yellow” form compared to 33.5° for the “green” form)^[17] gives stronger intermolecular interaction in the stacked pairs of complexes that results in 22 nm bathochromic shift in the solid-state emission band of the “yellow” form (576 nm, Figure S2) compared to the “green” one (554 nm, Figure S2). Expectedly, both forms gave identical emission spectra with the maxima at ca. 560 nm in dilute THF solutions where the solid-state packing effects are not operative.

To vary the chemistry of micellar cores, we have chosen three block copolymers composed of the same hydrophilic poly(ethylene glycol) (PEG) block and three different hydrophobic blocks (Scheme 1b): poly(ϵ -caprolactone) (PCL₄₅-*b*-PEG₁₂₅, BC1), poly(1,4-butadiene) (PBD₉₀-*b*-PEG₁₃₀, BC2), and polystyrene (PS₃₅-*b*-PEG₁₁₅, BC3). BC2 and BC3 are commercial block copolymers, which were exhaustively characterized in our previous publication,^[24] while BC1 is a newly prepared analog of commercial PCL₄₅-*b*-PEG₁₁₅ characterized in the same article^[24] (Experimental section contains a detailed description of its preparation and characterization). The choice of these block copolymers was based on the following reasons: i) all the block copolymers (including the commercial analog of BC1) were shown to form compact (with hydrodynamic radii, R_h , less than 16 nm), massive (with molecular weights ranging from 1.1 to 2.4×10^6 g/mol) and non-cytotoxic micelles with low apparent critical micelle concentration ranging from 1.4 to 14 mg/L;^[24] ii) the commercial analog of BC1 was shown to effectively stabilize AIPE-active [Pt(C[^]N[^]*N[^]C[^])] complex inside its micelles and support aggregation and emergence of AIPE;^[20] iii) BC2 contains polybutadiene blocks that are quite flexible and potentially cross-linkable to form non-dissociating micelles, and iv) BC3 contains polystyrene blocks that form glassy cores (T_g of PS is ca. 104 °C)^[25] that lead to very stable (kinetically “frozen”)^[21,22] micelles. All possible PtX:BCY pairs (i.e., 12 different PtX@BCY systems, with $X = 1-4$ and $Y = 1-3$) were prepared and characterized for their “general” (loading efficiency, hydrodynamic sizes, and cytotoxicity) and photophysical properties (absorption, excitation, and luminescence spectra; QY values).

2.2. Preparation and General Characterization of Phosphorescent Block Copolymer Micelles

Block copolymer micelles loaded by PtX complexes were prepared by the solvent exchange method followed by dialysis against twice distilled water using the general protocol developed recently for similar system^[20] with one substantial optimization: here we used *N*-methylpyrrolidone (NMP) as a common (starting) solvent in addition to *N,N*-dimethylformamide (DMF), which was used in the previous study (Table 1).^[20] The change of DMF for NMP was dictated by the formation of abundant precipitate upon the preparation of some PtX@BCY pairs that gives a very low loading of the complexes into the micelles. On the contrary, the use of NMP provided better solubility of the starting compounds to suppress undesired precipitation and increase loading. After preparation, the dispersions were centrifuged for 15 minutes at 15,000 rpm (20,000 g), and only sedimentally stable fractions were used for further investigation.

The Pt1–Pt4 loading (weight ratios) values were calculated through absorption spectra of lyophilizates redissolved in THF or DMF (see Supporting information for detailed protocol). The latter solvent was used for the PtX@BC2 systems because of BC2's poor solubility in THF. Table 1 summarizes experimentally determined PtX loadings into micelles as a function of starting mixture compositions (the targeted loading was 10 wt.% of PtX for all studied systems). Contrary to the previously reported sys-

tem, which revealed almost 100% loading efficiency,^[20] most of the new systems revealed low (54% or less) loading (Table 1), except for Pt2@BC1, Pt3@BC3, and Pt4@BC2, demonstrating loading in the range from 65% to 67%. The change of DMF for NMP improved loadings as it is exemplified for Pt1@BC1 system, where it results in Pt1 loading increase from 11 to 54 wt.%. However, even the use of NMP did not raise loading efficiencies to desirable 100%, which is most probably due to unwanted concomitant precipitation of the complexes induced by the addition of water. Moreover, we noted that PtX loadings demonstrated rather poor batch-to-batch reproducibility, pointing to the influence of various kinetic factors on the exact ratio between the rates of complexes precipitation and their embedding into micelles.

The study of PtX@BCY systems by dynamic light scattering (DLS) demonstrated (Table 1) that the micelles loaded by Pt(II) complexes revealed rather small size (R_h values did not exceed 23 nm for PtX@BC1, 15 nm for PtX@BC2, and 20 nm for PtX@BC3), which is only slightly higher than those of the parent “empty” micelles (22, 12.9,^[24] and 13.7^[24] nm for BC1, BC2, and BC3, respectively). These observations are completely in line with our previous reports showing almost negligible loading effect on the size of micelles.^[20,26] It is also worth noting that only the PtX@BC1 systems demonstrated unimodal size distributions (Figure S3), while all other systems featured bimodal ones (Figures S4 and S5), where the appearance of the slow mode demonstrated almost negligible concentration dependence (Figure S6). The unimodal character of size distributions for PtX@BC1 systems allowed calculations of polydispersity index (PDI) values. PDI values ranged from 0.009 to 0.392 (Table S3) featuring rather high variations between different micelle types but demonstrating narrow size distributions for all the PtX@BC1 systems. This is in full agreement with the observations made previously for “empty” micelles based on the same BC2 and BC3 block copolymers as well as on the commercial analog of BC1.^[24] Most probably, the bimodality is due to secondary micellar aggregation, which, however, does not play an important role in the chemistry of the studied systems, as the estimated weight fraction of these aggregates is well below 1%, as it was found earlier for the corresponding “empty” micelles based on BC2 and BC3 block copolymers.^[24]

2.3. Photophysical Investigation of the Phosphorescent Block Copolymer Micelles

Because the most pronounced photophysical evidence of the AIPE phenomenon demonstrated by the related [Pt(C[^]N[^]*N[^]C[^])]@PCL₄₅-*b*-PEG₁₁₅ system was the emergence of a new bathochromically shifted emission band,^[20] we started with the measurement of emission spectra for the PtX@BCY systems (Figure 1), which displayed several major effects. First, one can observe that both complexes prone to AIPE in the water/THF mixtures (Pt1 and Pt2) also demonstrate this effect in the BC1-based micelles. In addition to the major emission band, which is evidently due to the emission of the non-aggregated chromophores, the spectra of these systems display the devel-

Table 1. Loadings and loading efficiencies, R_h values, and quantum yields for PtX@BCY systems.						
PtX@BCY	Solvent	Theoretical Loading, wt. %	Experimental Loading, wt. %	Loading Efficiency, %	R_h , nm	QY(aer)/QY(deg), %
Pt1@BC1	DMF	10.9	1.2 ^{a)}	11	22	3.2/6.5
Pt1@BC1	NMP	10.2	5.5 ^{a)}	54	22	4.6/6.3
Pt1@BC2	NMP	10.0	3.5 ^{b)}	35	15 ^{d)}	0.5/1.1
Pt1@BC3	NMP	9.8	1.0 ^{a)}	10	17 ^{d)}	6.1/6.9
Pt2@BC1	DMF	10.4	6.8 ^{a)}	65	23	1.8/3.1
Pt2@BC2	NMP	10.4	2.2 ^{b)}	21	14 ^{d)}	0.2/0.3
Pt2@BC3	NMP	10.5	2.5 ^{a)}	24	18 ^{d)}	0.7/1.6
Pt3@BC1	NMP	10.2	1.0 ^{a)}	10	21	0.4/0.8
Pt3@BC2	NMP	9.9	1.3 ^{b)}	13	13 ^{d)}	0.5/0.9
Pt3@BC3	NMP	10.4	6.8 ^{a)}	65	19 ^{d)}	2.5/4.0
Pt4@BC1	NMP	10.2	1.8 ^{a)}	18	22	0.5/1.1
Pt4@BC2	NMP	9.8	6.6 ^{b)}	67	13 ^{d)}	0.2/0.4
Pt4@BC3	NMP	10.2	5.4 ^{a)}	53	20 ^{d)}	1.6/2.6

^{a)}The loading was determined via absorbance of lyophilizate solution in THF.
^{b)}The loading was determined via absorbance of lyophilizate solution in DMF.
^{c)}Presented R_h values correspond the fast mode of bimodal size distribution.

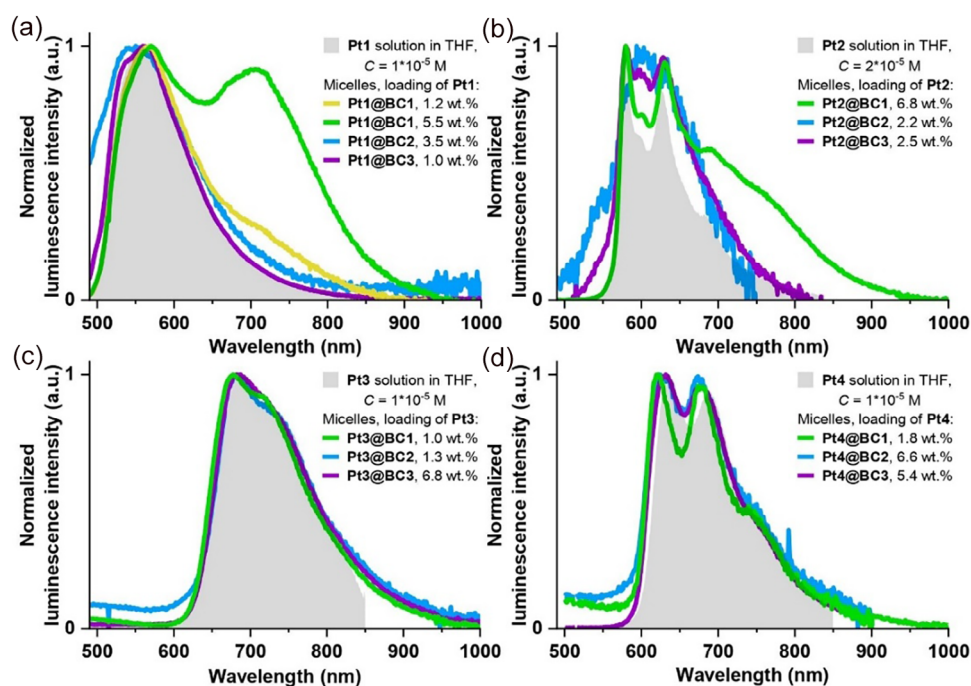


Figure 1. Emission spectra of the systems PtX@BCY in aqueous dispersions overlaid with emission spectra of the corresponding PtX in dilute THF solutions.

opment of a new feature appearing as a clearly discernible band at a high loading degree (5.5 wt.%) in the case of Pt1@BC1 (Figure 1a) and as shoulders at the major band for Pt1@BC1 at a low loading degree (1.2 wt.%) and for Pt2@BC1 (loading 6.8 wt.%; Figure 1b). It is also worth noting that in the case of Pt1@BC1, the new band centered at ca. 700 nm is very similar in its width and position to the bands that appeared in concentrated THF solutions of Pt1 (ca. 720 nm) or THF/water mixtures (ca. 680 nm).^[17]

The obtained spectroscopic data indicate that two types of chromophores exist inside the micelles, the photophysics of one of which (major emission band) is essentially similar to that of the isolated complexes in diluted solution and those in solid state, whereas the other can be assigned to the aggregated chromophores showing AIPE. One can also observe a slight bathochromic shift of the major peak (to ca. 570 nm) in the emission spectra of the Pt1@BC1 system (Figure 1a) compared to the spectra in THF. This indicates that packing of non-aggregated

chromophores in (Pt1@BC1) is closer to that of the “yellow” crystalline form (emission band maximum at 576 nm; *vide supra*) than to that observed for the “green” allotrope. In line with the previously described [Pt(C⁺N⁻N⁻C⁻)]@PCL₄₅-b-PEG₁₁₅ system,^[20] the emergence of AIPE did not lead to the appearance of any new bathochromically shifted absorption or excitation bands in the corresponding spectra (Figures S7 and S8). This observation indicates that excimer emission mechanism is operative for the aggregates in the Pt1@BC1 and Pt2@BC1, as it has been shown earlier for the closely related system.^[20]

Second, one can also note that the Pt3 and Pt4 complexes, which did not reveal AIPE in water/THF mixtures, do not demonstrate it either upon loading into BC1 micelles (Figure 1c,d). On the contrary, in the Pt3@BC1 and Pt4@BC1 systems, we observed a detectable (ca. 10–15 nm) hypsochromic emission band shifts compared to the THF solutions. The other Pt3@BCY and Pt4@BCY systems do not display any substantial spectral changes that are also indicative of the absence of AIPE.

Third, one can also observe that the emergence of AIPE upon loading of the same complex (Pt1 or Pt2) into different micelles was observed exclusively for BC1 micelles (Figure 1a,b).

Based on these observations, we can conclude that the Pt1@BC1 and Pt2@BC1 systems demonstrating AIPE are the most promising for application in biomedical luminescent microscopy as phosphorescent probes and sensors for physiological parameters. It is particularly important in view of their low cytotoxicity; one can see (Figure S9) that cell viability in Chinese hamster ovary (CHO-K1) cell monolayers is at the level of 90% or higher after 24 h of exposure to increasing concentrations up to 3.0 mg/mL for all the micelles investigated. This result further corroborates our previous reports on low cytotoxicity of block polymer micelles, both “empty”^[24] and loaded by various phosphorescent TMC.^[20,26]

Another common manifestation of AIPE is an increase in the phosphorescence QY values for the AIPE systems compared to their counterparts lacking this effect. To investigate this aspect, we performed determination of QY for all the prepared PtX@BCY systems (Table 1). Unexpectedly, we observed a substantially more complicated picture that goes far beyond a simple increase in QY values for AIPE-active systems (Pt1@BC1 and Pt2@BC1) compared to their analogs. Indeed, though Pt2@BC1 demonstrated the highest QY values among the other Pt2@BCY systems, Pt1@BC1 displayed QY values lower than Pt2@BC3. The latter situation seems to be more common since all other subgroups (except for Pt2@BCY subgroup) demonstrated the same trend: PtX@BC3 system displayed the highest QY and PtX@BC2 system showed the lowest one (note that QY of Pt3@BC1 was slightly lower compared to Pt3@BC2 but the difference between these systems is statistically insignificant since the experimental error of QY determination is of ca. 20%).

The observed effects can be explained using the following assumption: QY values of emitters strongly depend on the local rigidity of the microenvironment, and it seems that the rigidity of a matrix plays a more important role compared to the restriction of internal motion related to the AIPE phenomenon. If this assumption is correct, we can draw a much clearer picture. First, glassy PS cores (T_g of PS is ca. 104 °C)^[25] provide

the most rigid matrix in the series, and in all the cases except Pt2@BCY systems, this leads to the highest QY values. Second, molten PBd cores (T_m of PBd is ca. 1 °C)^[25] provide the flexible matrix, and in all the cases this results in the lowest QY values; in addition, PBd cores can quench excited states of triplet emitters due to non-radiative energy transfer to vibrational levels of C=C bond (this suggestion is supported by changed profiles of absorption and excitation spectra in the case of PtX@BC2, see Figures S7 and S8). Third, poly(ϵ -caprolactone) is semicrystalline but is plasticized by water^[27] and is expected to provide a less rigid matrix compared to PS; additionally, water present in the PCL matrix in substantial amounts can quench phosphorescence and lead to a further decrease in QY. The proposed explanation is generally consistent with the experimental observations but does not explain the behavior of the Pt2@BCY subgroup. Most probably, some specific interactions of Pt2 with different polymer matrices induce substantial changes in the QY values. Finally, from the comparison of QY values obtained in aerated and degassed solutions, we can conclude that there is no significant loss of oxygen sensitivity in the systems featuring the AIPE (QY(deg)/QY(aer) ratio varies from 1.2 to 2.1) compared to systems lacking it (QY(deg)/QY(aer) ratio varies from 1.1 to 2.3). These findings can serve as an additional argument toward the development of oxygen sensors based on AIPE-active emitters embedded into polymer micelles.^[20]

2.4. The AIPE Effect in Polymer Films

In view of the exceptional role of BC1 block copolymer micelles in supporting the AIPE phenomenon, we hypothesized that this effect is related to the ability of poly(ϵ -caprolactone) to swell in water to a rather substantial swelling degree (up to 2.5 vol.% at 37 °C).^[27] If this assumption is correct, one can suggest that the water content in the PCL core of BC1 micelles becomes high enough to induce the aggregation of highly hydrophobic Pt1 and Pt2 molecules, ultimately leading to the emergence of AIPE.

To validate this hypothesis, we studied the emission spectra of the Pt1/Pt3-doped PCL and PS films cast from THF or THF/water mixtures with water content of 10, 25, and 50 vol.% (Figure 2). Although the difference between the thickness of polymer film and the diameter of micellar core is up to three orders of magnitude, we believe that in both matrices the aggregation of Pt(II) complexes and the concomitant AIPE effect are confined to nanoscale. Consequently, at this scale, the microenvironments of the emitter molecule buried into the macroscopic film or, alternatively, into the micellar core can be essentially the same. The complexes and polymer matrices were chosen so that one complex (Pt1) and one matrix (PCL) were AIPE-active while their counterparts were not. The only system that demonstrated the desired AIPE was the Pt1 complex in PCL films obtained from the THF/water mixtures with 25 vol.% of water or more (Figure 2a). All changes in film preparation conditions (decrease in water content to 10 vol.% or less, substitution of PCL by PS or Pt1 by Pt3) resulted in the disappearance of AIPE (Figure 2). This observation allows concluding that the combination of an appropriate polymer matrix and high enough water

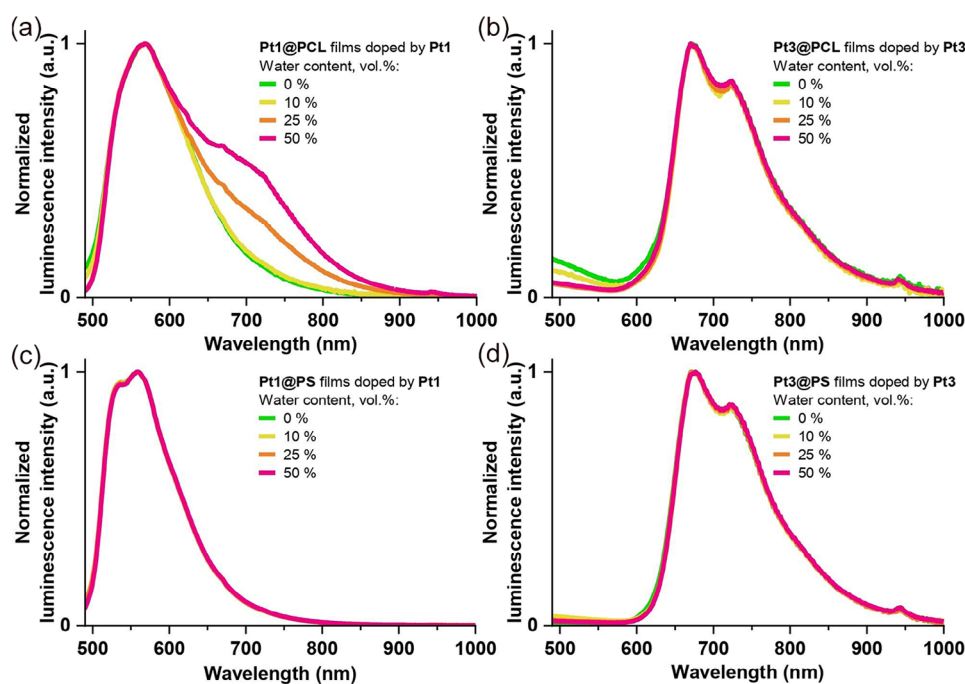


Figure 2. Luminescence spectra of PCL (a, b) and PS (c, d) films doped by Pt1 (a, c) and Pt3 (b, d). The films were cast from THF or THF/water with water content of 10, 25, and 50 vol.%.

concentration in the stock solution made it possible to observe AIPE. Indeed, on the one hand, in the absence of or at low contents of water, even the PCL matrix does not induce aggregation, while the increase in water content does. On the other hand, the PS matrix does not induce aggregation of Pt1 even in the presence of up to 50 vol.% of water, while the PCL matrix does. This means that the ability of PCL to incorporate water in amounts high enough to induce aggregation of AIPEgens is the key matrix characteristic that makes it possible to host aggregated AIPEgens in the micelles with PCL cores.

It is worth noting that λ_{MAX} of the Pt1@PCL major band is ca. 570 nm for all studied films. This value is identical to that of Pt1@BC1 micelles that is indicative of similarity in packing of “non-aggregated” Pt1 chromophores in PCL films and in polymer micelles.

The emergence of AIPE in PCL films may be ascribed to higher compatibility of PCL with water. In a four-component system (platinum complex, polymer, THF, and water) used for film casting, the hydrophobic complexes are concentrated in the vicinity of PCL. The presence of water, which is possible due to the higher affinity of PCL to water (compared to the hydrophobic PS), evidently provokes aggregation of Pt1 in a way suitable for the emergence of AIPE. However, this process competes with the sedimentation of a solid microphase, where the arrangement of chromophores does not allow AIPE. The balance between these simultaneous processes ultimately dictates the emergence of AIPE in PCL-based systems. In contrast, in the case of PS, the complete incompatibility of both polymer and Pt1 with water most probably results in phase separation, preventing the aggregation of Pt1 complexes and, consequently, the emergence of AIPE.

3. Conclusion

Finally, we can draw two major conclusions based on the data obtained. First, the influence of the properties of [Pt(C⁻N⁺N⁺C⁻)] complexes on the AIPE phenomenon is straightforward: if a particular complex is able to demonstrate AIPE in water-organic solvent mixtures, it also can demonstrate this effect upon loading into micelles. Complex planarity and steric bulkiness of its ligand environment determine its ability (or inability) to be packed into compact aggregates capable (or incapable) of demonstrating the AIPE phenomenon. Second, the influence of hydrophobic block chemistry is counterintuitive, since the only micelles that appeared to induce AIPE were those with poly(ϵ -caprolactone) cores. In view of this finding, we can speculate that PCL is the only block investigated in the study that can also swell in water, and water content in PCL cores is high enough to induce the complexes aggregation in a way suitable for the generation of AIPE. It is also worth noting that the discovered selectivity of the PCL matrix is manifested at both nanoscale (in micelle cores) and macroscopic level (in films), allowing us to conclude that it is the microenvironment of Pt(II) emitter that is responsible for the absence or emergence of aggregation and AIPE. Indeed, the investigation of the influence of micellar core on the emergence of AIPE should be continued and performed on a much broader library of block copolymers with special attention to amphiphilic core-forming blocks rather than to hydrophobic ones, including (but not limited to) those based on the other polyesters (poly lactides/glycolides, polyhydroxyalkanoates, etc.), hydrophobic poly(amino acids) (ranging from polyalanine to polyphenylalanine, polytryptophan, etc.), and amphiphilic polyethers (pluronics/ploxamers, etc.). Addi-

tionally, much broader study of the TMC structure and composition effects on the emergence of AIPE in polymer micelles and other polymer nanoparticles is still necessary. In this respect, other complexes of Pt(II) as well as Pd(II), Rh(I), Au(I), and Au(III) complexes should be investigated for their ability to demonstrate AIPE in water-organic mixtures and polymer micelles to pave the way to their application in biomedical research.

4. Experimental Section

4.1. General Comments

All the basic laboratory procedures and measurement protocols and experiments, such as micelles preparation, estimation of micelles loading by Pt1–Pt4 complexes by UV–vis absorption spectroscopy, dynamic light scattering, and photophysical experiments, as well as cell culture maintenance and a cell viability (MTT) assay, were performed using the protocols developed in our previous publication on phosphorescent micelles^[20] with slight modifications that are described in detail in the Supporting Information file. The newly developed experimental procedures are described below.

4.2. Synthesis and Characterization of PCL₄₅-*b*-PEG₁₂₅ Block Copolymer (BC1)

The diblock copolymer BC1 was prepared by ring-opening polymerization of ϵ -caprolactone, using monomethoxy poly(ethylene glycol), MeO-PEG-OH, as the macroinitiator and tin 2-ethylhexanoate, Sn(Oct)₂, as the catalyst (all the reagents were from Sigma-Aldrich). Prior to the synthesis, MeO-PEG-OH was dried in a vacuum over P₄O₁₀ for 1 week, ϵ -caprolactone was twice vacuum distilled, and Sn(Oct)₂ was used as received. The polymerization protocol consisted of heating overnight the flame-dried round-bottom flask containing MeO-PEG-OH (5.095 g; 1.02 mmol), ϵ -caprolactone (5.082 g; 44.5 mmol), and Sn(Oct)₂ (30 mg; 0.074 mmol) on an oil bath to 140 °C in an argon atmosphere. Then the reaction mixture was cooled down to room temperature. The resulting block copolymer was dissolved in methylene chloride and purified by precipitation and continuous washing with diethyl ether, after which the precipitated block copolymer was dried in a vacuum for 24 h at room temperature. The yield: 9.813 g (96.4%). The resulting BC1 was characterized by ¹H, ¹H–¹H COSY (Figure S10), ¹³C NMR (Figure S11), a combination of HMBC and HSQC spectra (Figure S12), and GPC (M_w = 16,900 g/mol; M_n = 11,500 g/mol; \mathcal{D} = 1.47; Figure S13A). Based on GPC data for starting MeO-PEG-OH (M_w = 6600 g/mol; M_n = 5500 g/mol; \mathcal{D} = 1.20; Figure S13B) and integration of ¹H NMR spectra, the calculated polymerization degrees of PCL and PEG blocks were 45 and 125, respectively.

4.3. Preparation of PtX-Doped Polymer Films

PCL and PS films doped with Pt1 and Pt3 complexes were cast from THF solutions with 10–50 vol.% or without added water. To prepare the films, stock solutions were first prepared by dissolving polymer-complex mixtures with a complex mass fraction of 2.5 wt.% in THF to a concentration of 100 mg/mL. For complete dissolution and dispersion of both components, the solution was sonicated in an ultrasonic bath for 2 h at 50 °C. Then, to cast films with a mass of 25 mg each, the necessary amounts of water (0, 10, 25, or 50 vol.% with respect to the final volume), THF, and 250 μ L of

stock solution were sequentially added onto a watch glass. The mixture was thoroughly stirred using a pipette tip and left to dry at room temperature for 24 h. The luminescence spectra of the films were obtained using an Avantes spectrofluorimeter and the AvaSoft software by a specialized probe designed for measuring the luminescence spectra of substances in the solid phase.

Supporting Information

The authors have cited additional references within the [Supporting Information](#).^[17,20,24,28–34] Deposition number 2390742 (for Pt1) contains the supplementary crystallographic data for this paper. These data are provided free of charge by the joint Cambridge Crystallographic Data Centre and Fachinformationszentrum Karlsruhe [Access Structures service](#).

Acknowledgements

This research was funded by the Russian Science Foundation, grant no. 24-23-00275, <https://rscf.ru/project/24-23-00275/>. The experimental studies were carried out using equipment of the Research Park of St. Petersburg State University (Centers for Magnetic Resonance, for X-ray diffraction studies, for Optical and Laser Materials Research, for Chemical Analysis and Materials Research, and for Diagnostics of Functional Materials for Medicine, Pharmacology, and Nanoelectronics, and Cryogenic division).

Conflict of Interests

The authors declare no conflict of interest.

Data Availability Statement

The data that support the findings of this study are available in the [Supporting Information](#) of this article.

Keywords: Aggregation-induced phosphorescence · Block copolymer micelle · Lifetime · Near-infrared luminescence · Tetradentate Pt(II) complexes

- [1] V. Sathish, A. Ramdass, P. Thanasekaran, K.-L. Lu, S. Rajagopal, *J. Photochem. Photobiol. C Photochem. Rev.* **2015**, *23*, 25–44.
- [2] L. Ravotto, P. Ceroni, *Coord. Chem. Rev.* **2017**, *346*, 62–76.
- [3] V. V. Sivchik, E. V. Grachova, A. S. Melnikov, S. N. Smirnov, A. Y. Ivanov, P. Hirva, S. P. Tunik, I. O. Koshevoy, *Inorg. Chem.* **2016**, *55*, 3351–3363.
- [4] Y. Zhu, K. Luo, L. Zhao, H. Ni, Q. Li, *Dye Pigment.* **2017**, *145*, 144–151.
- [5] S. Wang, K. Gu, Z. Guo, C. Yan, T. Yang, Z. Chen, H. Tian, W. H. Zhu, *Adv. Mater.* **2019**, *31*, 1805735.
- [6] S. Culham, P. H. Lanoë, V. L. Whittle, M. C. Durrant, J. A. G. Williams, V. N. Kozhevnikov, *Inorg. Chem.* **2013**, *52*, 10992–11003.
- [7] J. Lin, C. Zou, X. Zhang, Q. Gao, S. Suo, Q. Zhuo, X. Chang, M. Xie, W. Lu, *Dalton Trans.* **2019**, *48*, 10417–10421.
- [8] A. K. W. Chan, K. M. C. Wong, V. W. W. Yam, *J. Am. Chem. Soc.* **2015**, *137*, 6920–6931.

- [9] J. Wang, J. J. Nie, P. Guo, Z. Yan, B. Yu, W. Bu, *J. Am. Chem. Soc.* **2020**, *142*, 2709–2714.
- [10] D. Jaque, L. Martínez Maestro, B. Del Rosal, P. Haro-Gonzalez, A. Benayas, J. L. Plaza, E. M. Rodríguez, J. García Solé, *Nanoscale* **2014**, *6*, 9494–9530.
- [11] P. Chen, T. J. Meyer, *Chem. Rev.* **1998**, *98*, 1439–1478.
- [12] J. V. Caspar, E. M. Kober, B. P. Sullivan, T. J. Meyer, *J. Am. Chem. Soc.* **1982**, *104*, 630–632.
- [13] J. V. Caspar, T. J. Meyer, *J. Phys. Chem.* **1983**, *87*, 952–957.
- [14] C. A. Strassert, C. Chien, M. D. Galvez Lopez, D. Kourkoulos, D. Hertel, K. Meerholz, L. De Cola, *Angew. Chem. Int. Ed.* **2011**, *50*, 946–950.
- [15] S. R. Barzegar-Kiadehi, M. Golbon Haghighi, M. Jamshidi, B. Notash, *Inorg. Chem.* **2018**, *57*, 5060–5073.
- [16] G. Romo-Islas, S. Burguera, A. Frontera, L. Rodríguez, *Inorg. Chem.* **2024**, *63*, 2821–2832.
- [17] A. I. Solomatina, E. E. Galenko, D. O. Kozina, A. A. Kalinichev, V. A. Baigildin, N. A. Prudovskaya, J. R. Shakirova, A. F. Khlebnikov, V. V. Porsev, R. A. Evarestov, S. P. Tunik, *Chem. A Eur. J.* **2022**, *28*, e202202207.
- [18] I. Maisuls, C. Wang, M. E. Gutierrez Suburu, S. Wilde, C.-G. Daniliuc, D. Brünink, N. L. Doltsinis, S. Ostendorp, G. Wilde, J. Kösters, U. Resch-Genger, C. A. Strassert, *Chem. Sci.* **2021**, *12*, 3270–3281.
- [19] S. Liu, H. Sun, Y. Ma, S. Ye, X. Liu, X. Zhou, X. Mou, L. Wang, Q. Zhao, W. Huang, *J. Mater. Chem.* **2012**, *22*, 22167–22173.
- [20] N. A. Zharskaia, A. I. Solomatina, Y.-C. Liao, E. E. Galenko, A. F. Khlebnikov, P.-T. Chou, P. S. Chelushkin, S. P. Tunik, *Biosensors* **2022**, *12*, 695.
- [21] J. F. Gohy, *Adv. Polym. Sci.* **2005**, *190*, 65–136.
- [22] G. Riess, *Prog. Polym. Sci.* **2003**, *28*, 1107–1170.
- [23] Y. Liu, X. Chen, X. Liu, W. Guan, C. Lu, *Chem. Soc. Rev.* **2023**, *52*, 1456–1490.
- [24] A. A. Elistratova, A. S. Gubarev, A. A. Lezov, P. S. Vlasov, A. I. Solomatina, Y.-C. Liao, P.-T. Chou, S. P. Tunik, P. S. Chelushkin, N. V. Tsvetkov, *Polymers (Basel)* **2022**, *14*, 4361.
- [25] J. Brandrup, E. H. Immergut, E. A. Grulk, *Polymer Handbook*, 4th ed., John Wiley & Sons Ltd., Hoboken, **1999**.
- [26] A. A. Elistratova, I. S. Kritchenkov, A. A. Lezov, A. S. Gubarev, A. I. Solomatina, D. V. Kachkin, N. A. Shcherbina, Y.-C. Liao, Y.-C. Liu, Y.-Y. Yang, N. V. Tsvetkov, P. S. Chelushkin, P.-T. Chou, S. P. Tunik, *Eur. Polym. J.* **2021**, *159*, 110761.
- [27] D. Łysik, J. Mystkowska, G. Markiewicz, P. Deptuła, R. Bucki, *Polymers (Basel)* **2019**, *11*, 1880.
- [28] CrysAlisPro Software System, Version 1.171.41.94a; Rigaku Oxford Diffraction: Oxford, UK **2021**.
- [29] G. M. Sheldrick, *Acta Crystallogr. Sect. C Struct. Chem.* **2015**, *71*, 3–8.
- [30] G. M. Sheldrick, *Acta Crystallogr. Sect. A Found. Adv.* **2015**, *71*, 3–8.
- [31] O. V. Dolomanov, L. J. Bourhis, R. J. Gildea, J. A. K. Howard, H. Puschmann, *J. Appl. Crystallogr.* **2009**, *42*, 339–341.
- [32] A Guide to Recording Fluorescence Quantum Yields can be found under https://static.horiba.com/fileadmin/Horiba/Application/Materials/Material_Research/Quantum_Dots/quantumyieldstrad.pdf, **2020**.
- [33] A. M. Brouwer, *Pure Appl. Chem.* **2011**, *83*, 2213–2228.
- [34] T. Mosmann, *J. Immunol. Methods* **1983**, *65*, 55–63.

Manuscript received: December 04, 2024